Title	Development and application of a method for discriminating the influence of radon progenies in air from aerial radiation monitoring data
Author(s)	Hirouchi Jun, Nishizawa Yukiyasu, Urabe Yoshimi, Shimada Kazumasa, Sanada Yukihisa, Munakata Masahiro
Citation	Applied Radiation and Isotopes,141,p.122-129
Text Version	Accepted Manuscript
URL	https://jopss.jaea.go.jp/search/servlet/search?5061336
DOI	https://doi.org/10.1016/j.apradiso.2018.08.027
Right	© 2018. This manuscript version is made available under the CC-BY-NC-ND 4.0 license http://creativecommons.org/licenses/by-nc-nd/4.0/. This is the accepted manuscript version. The formal published version is available at https://doi.org/10.1016/j.apradiso.2018.08.027.

Title

Development and application of a method for discriminating the influence of radon progenies in air from aerial radiation monitoring data

Author names and affiliations

Jun Hirouchi [a,*], Yukiyasu Nishizawa [b], Yoshimi Urabe [c], Kazumasa Shimada [a], Yukihisa Sanada [d], Masahiro Munakata [a]

[a] Nuclear Safety Research Center, Japan Atomic Energy Agency, 2-4 Shirane Shirakata, Tokai-mura, Naka-gun, Ibaraki 3191195, Japan

[b] OYO Corporation, 1-66-22 Miyahara-cho, Kita-ku, Sitama-shi, Saitama, 3310812, Japan.

[c] NESI Inc., 38 Shinko-cho, Hitachinaka, Ibaraki, 3120005, Japan.

[d] Fukushima Remote Monitoring Group, Fukushima Environmental Safety Center, Japan Atomic Energy Agency, 45-169 Sukakeba, Kaihama-aza, Haramachi-ku, Minami-soma, 9750036, Japan.

*Corresponding author, E-mail address: hirouchi.jun@jaea.go.jp (Jun Hirouchi)

Abstract

The influence of gamma-rays from natural nuclides (particularly the radon progenies, ^{214}Pb and ^{214}Bi) must be excluded from aerial radiation monitoring (ARM) data to accurately estimate the deposition of artificial radionuclides. A method for discriminating the influence of the radon progenies in air from the ARM data was developed. Two types of detectors with different crystal sizes were installed in a helicopter. The gamma-ray responses of these detectors were simulated using EGS5. The influence of the radon progenies in air was excluded using the relation between the count rates of six NaI (Tl) detectors and a $LaBr_3$ detector. The discrimination method was applied to the ARM data obtained from around the Sendai and Fukushima Dai-ichi Nuclear Power Stations. To verify the validity of the discrimination method, the dose rate estimated from the ARM data was compared with the dose rate measured using a NaI survey meter at a height of 1 m above the ground. The application of the discrimination method improved the dose rate estimation, showing the validity of the discrimination method.

Keywords

Aerial radiation monitoring, NaI(Tl) detector, $LaBr_3$ detector, Radon progeny

1. Introduction

Aerial radiation monitoring (ARM) using a helicopter is one of the most effective methods for measuring the distribution of radioactivity deposited after nuclear accidents. In Japan, ARM was started as a national project to map the ground surface distribution of radiocesium after the Fukushima Dai-ichi Nuclear Power Station (NPS) accident (Lyons and Colton, 2012; Blumenthal, 2012). The ARM data provided basic information for the planning of evacuation zones and assessing the consequences and emergency countermeasures after the accident.

The ARM system uses detectors to measure the gamma-rays from the ground and air (Fig. 1). The sources of gamma-rays can be categorized into artificial and natural radionuclides. The spectral information obtained with the detectors used in the ARM system is difficult to distinguish the gamma-ray sources because ^{214}Bi, which belongs to the U-series, exhibits similar gamma-ray energy to that of radioactive cesium (^{134}Cs and ^{137}Cs). Therefore, gamma-rays from natural radionuclides interfere with the estimates of the amounts of deposited artificial radionuclides. Hendricks and Riedhauser (1999) and Sanada et al. (2014) divided the measured gamma ray spectra into two parts, artificial and natural indexes, to estimate the dose rate of natural and artificial radionuclides. The estimated dose rate of natural radionuclides was generally in agreement with the in-situ measured dose rate, showing the validity of the discriminating method. However, the estimated dose rate of the artificial radionuclides increased with time in some places, whereas it declined with time in other places because of physical decay. The inexplicable change over time can be caused by the influence of the radon progenies, ^{214}Pb and ^{214}Bi. The air concentration of the radon progenies can range from approximately 0 to more than 20 Bq m^{-3} in Japan because the air concentration depends on the height of the atmospheric mixed layer and the origin of air, i.e., continental or marine origin (Shimo et al., 2007). In addition, the radon concentration in air is different among different countries and ranges from 7 to 184 Bq m^{-3} (Zielinski and Chambers, 2008). Therefore, the influence of the radon progenies in air on the dose rate measurements needs to be understood. The influence from measurement data must be excluded to estimate the dose rates more accurately, not only for artificial radionuclides but also for natural radionuclides (background). To discriminate between radiation from the atmosphere and from the ground, the use of secondary detectors placed on top of the main detectors was suggested, known as the upward-looking detector method (IAEA, 1991; IAEA, 2003). In this paper, the influence of radon progenies in air is discriminated from ARM data based on the upward-looking detector method.

NaI(Tl) detectors have been used in ARM. In the first few weeks after release, however, the low resolution of a NaI(Tl) detector and the coexistence of ^{132}I can cause erroneous Cs concentration estimation (Hirouchi et al., 2015). In Japan, a $LaBr_3$ detector, which has high energy resolution and efficiency, has been used recently in ARM to resolve inaccurate estimates. However, it is difficult to apply the upward-looking detector method to a pulse height distribution measured by a $LaBr_3$ detector because the inherent contamination of a $LaBr_3$ detector influences the energy range used in the upward-looking detector method and can cause poor estimate accuracy.

The aim of this study is to develop a method for discriminating the influence of radon progenies in air from ARM data with NaI(Tl) detectors and a $LaBr_3$ detector. The influence of radon progenies in air was excluded from the relation between the count rates of six NaI (Tl) detectors and a $LaBr_3$ detector. The method is applied to the ARM data around the Sendai and Fukushima Dai-ichi NPSs. The discrimination method can be used to obtain the air concentration of ^{222}Rn, which is the parent nuclide of ^{214}Pb and ^{214}Bi, from the ARM data; this method can provide useful information for understanding the atmospheric transport process because ^{222}Rn is used as a tracer gas for transport modelling (Hirao et al., 2008).

2. Theory and methods

2.1 ARM system

The ARM relied on a dedicated radiation detection system (RSX-3, Radiation solution Inc., Canada) installed on a manned helicopter. Six NaI(Tl) detectors (2" × 4" × 16") and one $LaBr_3$ detector (3" × 3") were mounted in the helicopter. The $LaBr_3$ detector was placed on the NaI(Tl) detectors. The arrangement of the detectors allowed the gamma-rays to attenuate into the $LaBr_3$ detector from the ground and provided the difference of the contribution ratio of gamma-rays from the ground and air between the NaI(Tl) and $LaBr_3$ detectors. The ARM system acquired a once-per-second readout of its spectrometers to produce a 1024-channel energy spectrum with 3 keV per channel. The spectrometer readings were synchronized with time from a global positioning system (GPS) receiver. The spectrum and GPS data (date, time, latitude, longitude, and height above the ellipsoid) were recorded every second. The spectrum data was calculated using the parameters such as an attenuation factor and a conversion factor of the dose rate at a height of 1 m, and the calculated data was compared with the measured dose rates. In the traditional method, the dose rate was calculated using the total count rate (C_{all}), whereas in the new method, it was calculated using only the count rate from the ground (C_g).

2.2. Discrimination theory

IAEA (1991) proposed that the contribution of ^{214}Bi (609 keV) to ^{137}Cs (662 keV) was subtracted using counts in the 1764 keV, which is a peak of ^{214}Bi. However, counts in the 1764 keV was too low to apply the method to the spectral information in Japan because of the flight height of approximately 300 m and the measurement time of 1 s. In the present study, we attempted to use the difference in response of the up and down-looking (one $LaBr_3$ detector and six NaI(Tl) detectors, respectively) . An NaI detector is able to use as up-looking detector in substitution for $LaBr_3$ detector because all count rate is applied in this method. The method for discriminating the influence of the radon progenies in air from ARM data was derived from the following four equations:

$$C_{NaI,all} = C_{NaI,g} + C_{NaI,a} \quad , \qquad (1)$$

$$C_{LaBr,all} = C_{LaBr,g} + C_{LaBr,a} \quad , \qquad (2)$$

$$R_a = \frac{C_{NaI,a}}{C_{LaBr,a}} \quad , \qquad (3)$$

$$R_g = \frac{C_{NaI,g}}{C_{LaBr,g}} \quad , \qquad (4)$$

where C is the count rate in the energy range of 100–700 keV. The influence of inherent contamination of a $LaBr_3$ detector is small, and R is the count rate ratio (C_{NaI}/C_{LaBr}); the subscripts NaI and $LaBr$ indicate the NaI(Tl) and $LaBr_3$ detectors, respectively, g is the contribution of the gamma-rays from the ground, a is the contribution of gamma-rays from the radon progenies in air, and *all* is both the contribution of the gamma-rays from the ground and air (g+a). Here, the background count rate is subtracted from C, which includes the contributions of cosmic-rays and contamination from the helicopter. In this study, the minimum count rate measured over the sea was used as the background count rate. The substitution of Eq. (3) into Eq. (1) leads to

$$C_{NaI,g} = C_{NaI,all} - R_a C_{LaBr,a} \quad , \tag{5}$$

the substitution of Eq. (2) into Eq. (5) leads to

$$C_{NaI,g} = C_{NaI,all} - R_a\left(C_{LaBr,all} - C_{LaBr,g}\right) \quad , \tag{6}$$

the substitution of Eq. (4) into Eq. (6) leads to

$$C_{NaI,g} = C_{NaI,all} - R_a\left(C_{LaBr,all} - \frac{C_{NaI,g}}{R_g}\right) \quad , \tag{7}$$

and Eq. (7) should be modified as

$$C_{NaI,g} = \frac{\left(C_{NaI,all} - R_a C_{LaBr,all}\right) R_g}{R_g - R_a} \quad . \tag{8}$$

Eqs. (1) and (8) show that the contribution of the radon progenies ($C_{NaI,\,a}$) can be discriminated using the total count rates of the NaI(Tl) and $LaBr_3$ detectors ($C_{NaI,\,all}$, $C_{LaBr,\,all}$) and the count rate ratio (R_a, R_g). In this study, R_a and R_g were determined using the ARM data and the computational calculations discussed in sections 2.3 and 2.4.

2.3. ARM data

To determine R_a and R_g, ARM was conducted around the Fukushima Dai-ichi and Sendai NPSs in

February, 2016 (Fig. 2 (a) and (b)). The ARM data at the Sendai NPS was applied to validate the discrimination method. Additionally, the ARM data over the area more than 80 km away from the Fukushima Dai-ichi NPS shown in Fig. 2 (c) was also applied to validate the discrimination method. The ARMs near the Fukushima Dai-ichi NPS (Fig. 2 (a)) were conducted multiple times over the same measurement lines, whereas those around the Sendai NPS and more than 80 km for the Fukushima Dai-ichi NPS were conducted once per measurement line in Fig. 2 (b) and (c). The height of the helicopter above the ground and sea was approximately 300 m.

2.4. Calculation of detector response

The conversion factors from the count rate to the air concentration of the radon progenies Γ (Bq m^{-3} cps^{-1}) and R_a were calculated using the Monte Carlo photon transport code EGS5 (Hirayama et al., 2005). The calculation geometry comprised a 1.3-km thick air layer, a 1-m thick soil or sea layer, and a helicopter model mounted six NaI(Tl) detectors and a $LaBr_3$ detector. The density of the air was set to be 1.2×10^{-3} g cm^{-3}. The soil composition and density were assumed to be pure SiO_2 and 1.6 g cm^{-3}, respectively. The sea composition and density were assumed to be pure H_2O and 1.0 g cm^{-3}, respectively. The horizontal size of the calculation domain was 1 km × 1 km with the detector at the center, supporting approximately 95% of a virtually infinite horizontal extent. The soil or sea layer was assumed to be flat, without considering the geometric structures and ground surface undulations such as mountains. The height of the helicopter model above the ground or sea was set to be 300 m so that the ARM could be reproduced. The diagram of the helicopter model is shown in Fig. 3. The helicopter was simply modeled using an ellipsoid made of 5-mm thick pure aluminum (2.7 g cm^{-3}).

Machines in the cockpit and the fuels were simply modeled using a pure aluminum cylinder and three kerosene cylinders, respectively; these cylinders largely attenuate gamma-rays. The composition and density of kerosene were assumed to be $C_{11}H_{24}$ and 0.81 g cm^{-3}, respectively. In contrast, other objects in the helicopter, such as chairs and floor plates, were not modeled because they exhibited lower attenuation of gamma-rays. The detailed constructions such as sizes and location of the detectors were considered to reproduce the ARM system.

The validation of the helicopter model was confirmed before calculating the conversion factor and R_a. The shielding effect of the helicopter was investigated using a checking source of ^{137}Cs. The detector responses were measured after setting the checking source on all the outer sides of the helicopter. The experimental results were compared with the calculation results that modeled the experimental situations. The ratio of the calculated to measured total count rates is shown in Fig. 4. This ratios on any positions of the checking source are approximately 1, and the helicopter model is valid.

The conversion factors of the NaI(Tl) and $LaBr_3$ detectors (Γ_{NaI}, Γ_{LaBr}) were calculated assuming that the radionuclides in air were uniformly distributed and the radioactive equilibrium between ^{214}Pb and ^{214}Bi was achieved. The count rate ratio R_a was calculated as the ratio of conversion factors between the NaI(Tl) and $LaBr_3$ detectors ($\Gamma_{LaBr}/\Gamma_{NaI}$). The calculated R_a was 27. The value of R_a was compared with the measurement data given in section 3.1.

2.5. Ground measurement for confirming the reliability of ARM data

In order to validate the measurement results of the ARM, they were compared to ground-based measurements at a height of 1 m that we performed with a NaI survey meter (TCS-172B, Hitachi Inc., Tokyo, Japan). We obtained air dose rate data at 28 points and 298 surrounding the Sendai NPS and the Fukushima Dai-ichi NPS shown in Fig. 2 (b) and (c), respectively. The air dose rate of the ground data (D_g) and the airborne data (D_a) were compared by visualizing the unevenness using a scatter diagram. The relative deviation (*RD*) of each measurement cell was calculated as follows in order to evaluate the accuracy of the ARM:

$$RD = \frac{D_a - D_g}{D_g} \quad . \tag{9}$$

Calculated *RD*s were used to evaluate the total error and statistical uncertainty, which is shown as a histogram of frequency. In addition, the difference between D_g and D_a was quantified using the normalized mean square error (*NMSE*) method for a relative evaluation between data sets. The *NMSE* was derived as follows:

$$NMSE = \frac{\sum_{i=1}^{n}\left(D_{g,i} - D_{a,i}\right)^2}{\sum_{i=1}^{n} D_{g,i}^2} \quad , \tag{10}$$

where *n* is the total number of data points.

3. Results and discussion

3.1. Count rate ratio, R_a and R_g

The relations between C_{NaI} and C_{LaBr} over the ground and sea are shown in Fig. 5. The ARM over the ground identified radionuclides in the soil as the gamma-ray source, whereas that over the sea identified the radon progenies in air as the gamma-ray source. Hence, the measured count rate ratio over the ground and the sea can be regarded as R_g and R_a, respectively. As shown in Fig. 5, the value of R_g is greater than R_a. This trend is caused by the difference in the contribution ratio of the gamma-ray sources owing to the detector arrangement.

If the values of R_g and R_a are different among places, those need to be preliminarily determined in each place. As shown in Fig. 5, both the values of R_g and R_a obtained from the ARM around the Sendai and Fukushima Dai-ichi NPSs are almost similar, although artificial radionuclides existed around the Fukushima Dai-ichi NPS. The result implies that the same R_a of 27 and R_g of 34 can be used at any place. In addition, the measured R_a is the same as the calculated R_a as described in section 2.3. This shows that an R_a of 27 can be certainly used at any place.

3.2. Application of the discrimination method

With the R_a and R_g determined in the last section, the discrimination method was applied to the ARM data around the Sendai NPS. The estimated dose rate map at a height of 1 m above the ground, before and after the application of the discrimination method, and the estimated air concentration map of the radon progenies are shown in Figs. 6 and 7, respectively. The air concentration was estimated with the product of the conversion factors Γ_{NaI} and the contribution of the radon progenies $C_{NaI,\,a}$ that was calculated by the discrimination method. The estimated air concentration map is not always the same as shown in Fig. 7 because the radon concentration in air fluctuates with time. A seamless digital geological map is shown in Fig. 8 (Geological Survey of Japan, AIST, 2015), which shows the locations at which large amounts of natural radionuclides are present. The comparison between Figs. 6(c) and 7 shows that the dose rate significantly decreased at the locations that were estimated to exhibit a high air concentration of the radon progenies. A radon air concentration of 10 Bq m^{-3}

caused an error of approximately 20 nSv h^{-1} in the calculated 1-m-height dose rate. The dose rate map before the application of the discrimination method (Fig. 6(a)) has almost the same pattern as that of the seamless digital geological map (Fig. 8). The application of the discrimination method improved the accuracy of the dose rate at the location indicated by dashed circles in Fig. 6(b), where the radon concentration was estimated to be higher. The validity of the discrimination method was verified by comparing the dose rate measured at a height of 1 m above the ground using a NaI survey meter with the one estimated using the ARM data before and after the application of the discrimination method (Fig. 9). Figure 9 shows also the frequent distribution of *RD*. The *NMSE* and the frequent distribution of *RD* were improved by applying the discrimination method. The results confirm the validity of the discrimination method.

Additionally, the method was applied to the ARM data over the area more than 80 km away from the Fukushima Dai-ichi NPS in 2016. The estimated dose rate maps at a height of 1 m above the ground, before and after the application of the discrimination method, are shown in Fig. 10. Figure 11 shows the comparison between the dose rate of ground data and ARM data as well as the frequent distribution of *RD*, before and after the application of the discrimination method. Radiocesium released from the Fukushima Dai-ichi NPS existed on a part of this area at the measurement time. In the high dose area surrounded by yellow circles in Fig. 10, the difference between the dose rate before and after the application of the discrimination method was little or none because the contribution of gamma-rays from air was relatively low compared to that from ground (Cs). In the low dose area surrounded by red dot circles in Fig. 10, on the other hand, the dose rate significantly decreased by applying the discrimination method. The results imply that the method is useful in the low dose area where the dose rate at a height of 1 m above the ground is less than 0.2 μSv h^{-1}. According to Fig.11, the dose rate of ARM data before applying the discrimination method tended to be larger than that of ground data. The *NMSE* and the frequent distribution of *RD* were improved by applying the discrimination method. The result shows also the validity of the discrimination method even in the area where radiocesium exists.

4. Conclusions

A method for discriminating the influence of the radon progenies in air from ARM data was proposed. The discrimination method used the relation between the count rates of NaI (Tl) detectors and a $LaBr_3$ detector. The dose rate map estimated after the application of the discrimination method was similar to the seamless digital geological map. In addition, to verify the validity of the discrimination method, the dose rate at a height of 1 m above the ground measured using a NaI survey meter was compared with the ARM data. The *NMSE* and the frequent distribution of *RD* were improved by applying the discrimination method. The results revealed that the discrimination method was valid. The discrimination method can be applied for measuring the ^{222}Rn concentration in air, which has rarely been conducted using the ARM. If we can measure the ^{222}Rn concentration in air, the atmospheric dispersion process and the wet deposition process could be investigated more detail with an atmospheric transport model. Therefore, the ARM will contribute not only to the assessment of the consequence after an accident but also to the resolution of the atmospheric transport process of nuclides.

Acknowledgements

This work was supported by the Nuclear Regulation Authority, Japan.

References

Lyones, C., Colton, D., 2012. Aerial measuring system in Japan, Health Phys. 102, 509–515.

Blumenthal, D.J., 2012. Introduction to the special issue on the U.S. Response to the Fukushima Accident, Health Phys. 102, 482–484.

Hendricks, T.J., Riedhauser, S.R., 1999. An Aerial Radiological Survey of the Nevada Test Site, DOE/NV/11718-324.

Sanada, Y., Sugita, T., Nishizawa, Y., Kondo, A., Torii, T., 2014. The aerial radiation monitoring in Japan after the Fukushima Daiichi nuclear power plant accident, Proc. Nucl. Sci. Technol. 4, 76–80.

Shimo, M., Yamasaki, K., Tsujimoto, T., Okamoto, K., Yoshimoto, T., Kojima, H., Mizuma, M., 2007. The influence of the concentration of atmospheric radon decay products on the environmental radiation dose rate. Japan Health Phys. Soc. 42(2), 156–165.

Zielinski, J. M., Chambers, D. B., 2008. Mapping of residential radon in the world, 2008 The 12th International Congress of the International Radiation Protection Association Buenos Aires, Argentina 19–24 October 2008.

IAEA, 1991. Airborne gamma ray spectrometer surveying. Technical Reports Series No. 323.

IAEA, 2003. Guidelines for radioelement mapping using gamma ray spectrometry data. IAEA-TECDOC-1363.

Hirouchi, J., Yamazawa, H., Hirao, S., Moriizumi, J., 2015. Estimation of surface anthropogenic radioactivity concentrations from NaI(Tl) pulse-height distribution observed at monitoring station. Radiat. Prot. Dosimet. 164, 304–315.

Hirao, S., Yamazawa, H., Moriizumi, J., Yoshioka, K., Iida, T., 2008. Development and verification of long-range atmospheric radon-222 transport model. J. Nucle. Sci. Technol. 45(Suppl. 6), 166–172.

Hirayama, H., Namito, Y., Bielajew, A.F., Wilderman, S.J., Nelson, W. R., 2005. The EGS5 Code System, KEK Report 2005-8, SLAC-R-730, High Energy Accelerator Reserch Organization (KEK), Stanford Linear Accelerator Center (SLAC).

Geological Survey of Japan, AIST (ed.). Seamless digital geological map of Japan 1: 200,000. May 29, 2015 version. Geological Survey of Japan, National Institute of Advanced Industrial Science and Technology. 2015.

Title

Development and application of a method for discriminating the influence of radon progenies in air from aerial radiation monitoring data

Fig. 1. Gamma-rays measured via aerial radiation monitoring.

Fig. 2. Measurement lines (a) around the Fukushima Dai-ichi NPS,(b) around the Sendai NPS, and (c) over the area more than 80 km away from the Fukushima Dai-ichi NPS.

Fig. 3. Diagram of the helicopter model.

Fig. 4. The ratio of the calculated to measured count rates in the experiment for investigating the shielding effect of the helicopter.

Fig. 5. Relation between C_{NaI} and C_{LaBr} (a) over the ground, (b) over the sea around the Sendai and Fukushima Dai-ichi NPSs.

Fig. 6. Dose rate maps at a height of 1 m calculated from the ARM data around the Sendai NPS. (a) before the discrimination; (b) after the discrimination; (c) the ratio of (b) to (a).

Fig. 7. Estimated air concentration map of the radon progenies around the Sendai NPS.

Fig. 8. Seamless digital geological map around the Sendai NPS (Geological Survey of Japan, AIST, 2015). The colored areas are places containing large amounts of natural radionuclides.

Fig. 9. Relation between the dose rates at a height of 1 m above the ground measured using a NaI survey meter and calculated from the ARM data around the Sendai NPS (a) before the discrimination (b) after the

discrimination. Frequency distribution of relative deviation around the Sendai NPS (c) before the discrimination (d) after the discrimination.

Fig. 10. Dose rate maps at a height of 1 m calculated from the ARM data around the Fukushima Dai-ichi NPS. (a) before the discrimination; (b) after the discrimination; (c) the ratio of (b) to (a).

Fig. 11. Relation between the dose rates at a height of 1 m above the ground measured using a NaI survey meter and calculated from the ARM data around the Fukushima Dai-ichi NPS (a) before the discrimination (b) after the discrimination. Frequency distribution of relative deviation around the Fukushima Dai-ichi NPS (c) before the discrimination (d) after the discrimination.

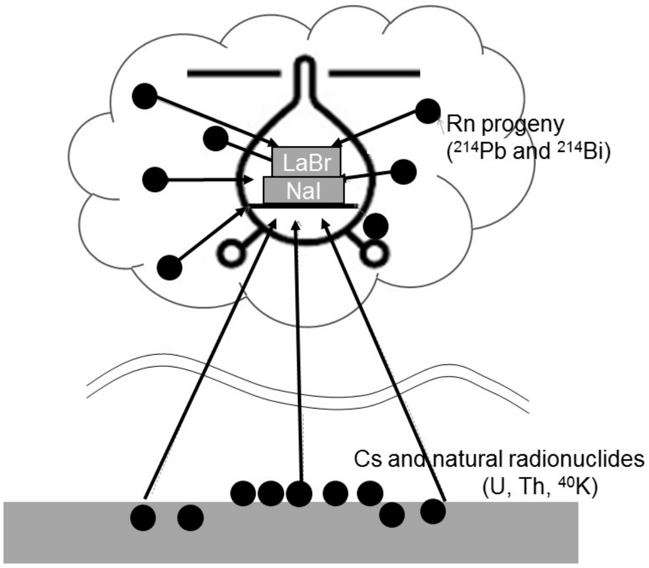

Fig. 1. Gamma-rays measured via aerial radiation monitoring.

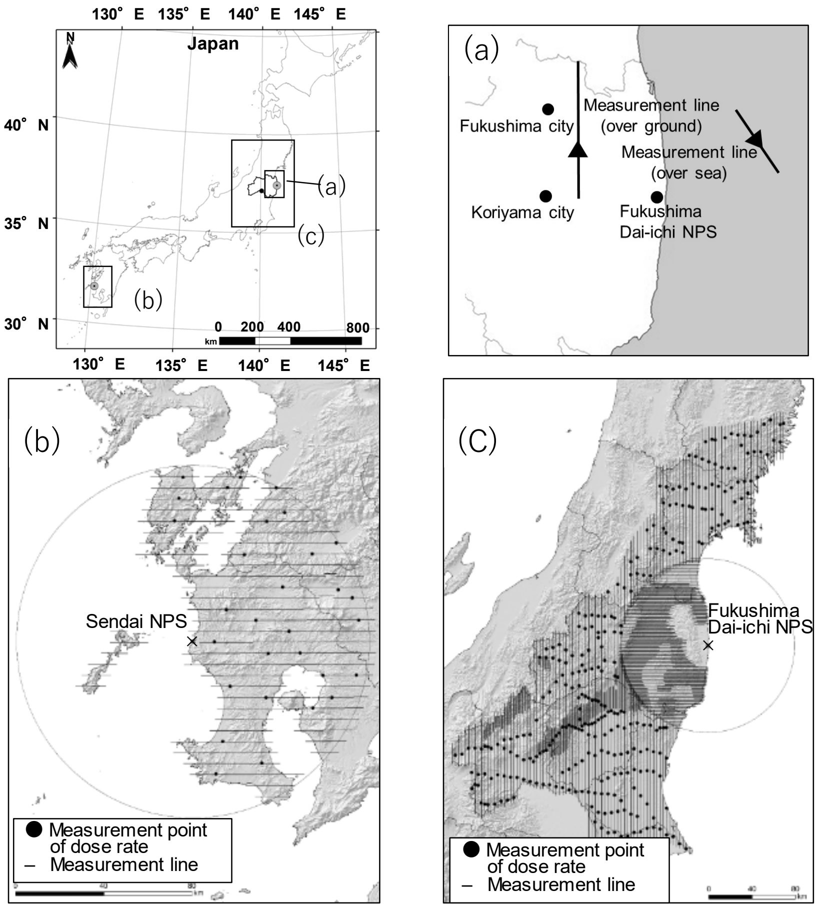

Fig. 2. Measurement lines (a) around the Fukushima Dai-ichi NPS,(b) around the Sendai NPS, and (c) over the area more than 80 km away from the Fukushima Dai-ichi NPS.

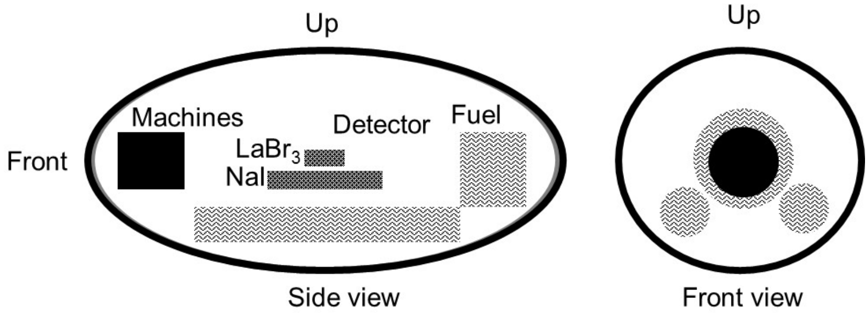

Fig. 3. Diagram of the helicopter model.

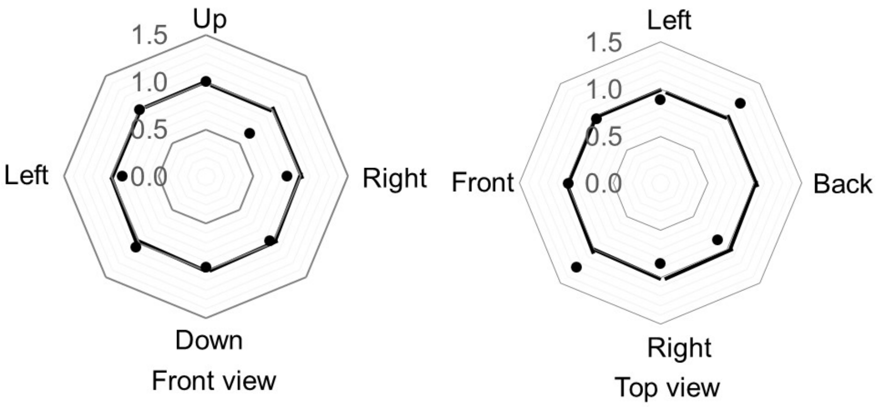

Fig. 4. The ratio of the calculated to measured count rates in the experiment for investigating the shielding effect of the helicopter.

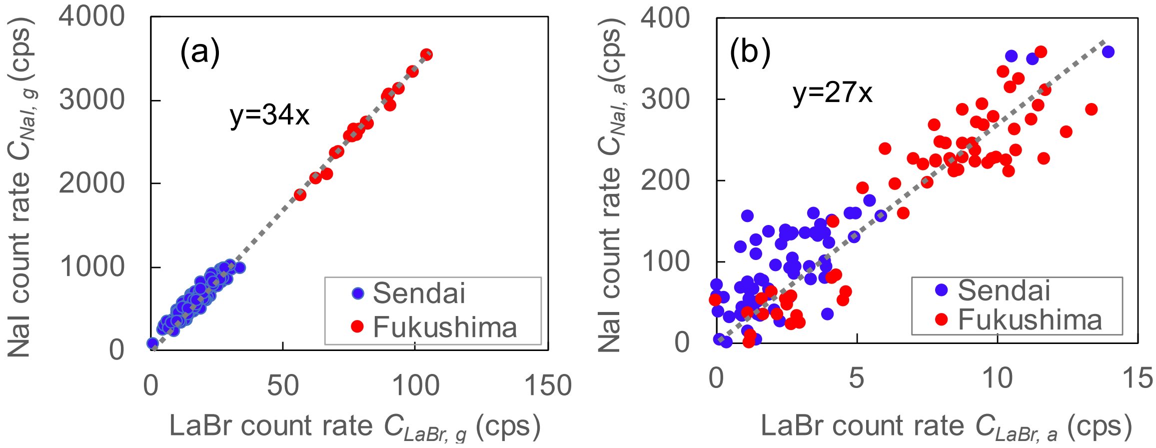

Fig. 5. Relation between C_{NaI} and C_{LaBr} (a) over the ground, (b) over the sea around the Sendai and Fukushima Dai-ichi NPSs.

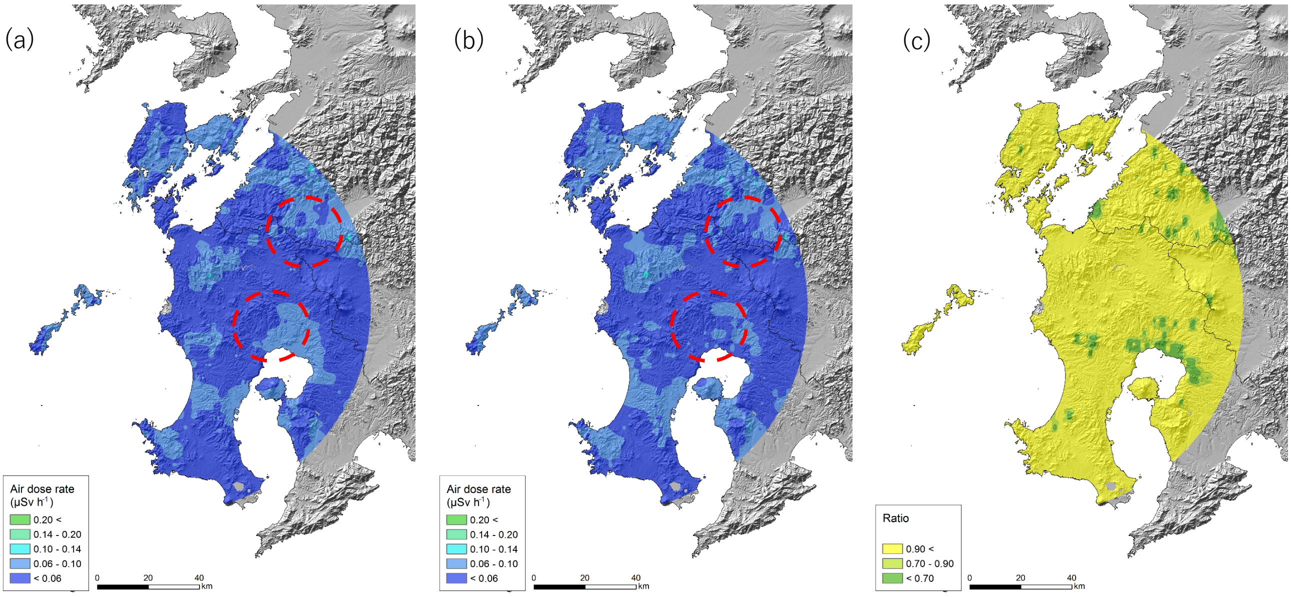

Fig. 6. Dose rate maps at a height of 1 m calculated from the ARM data around the Sendai NPS. (a) before the discrimination; (b) after the discrimination; (c) the ratio of (b) to (a).

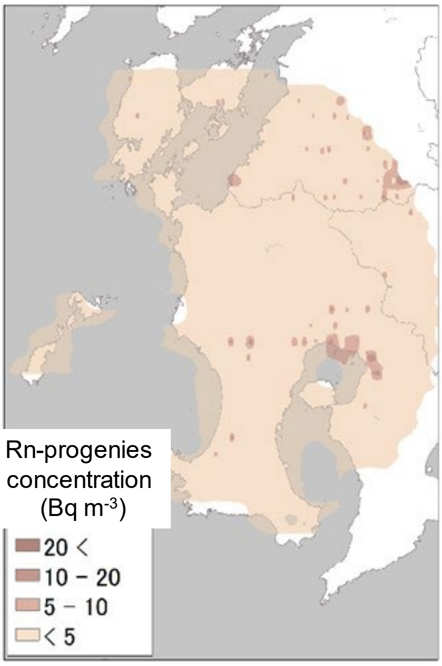

Fig. 7. Estimated air concentration map of the radon progenies around the Sendai NPS.

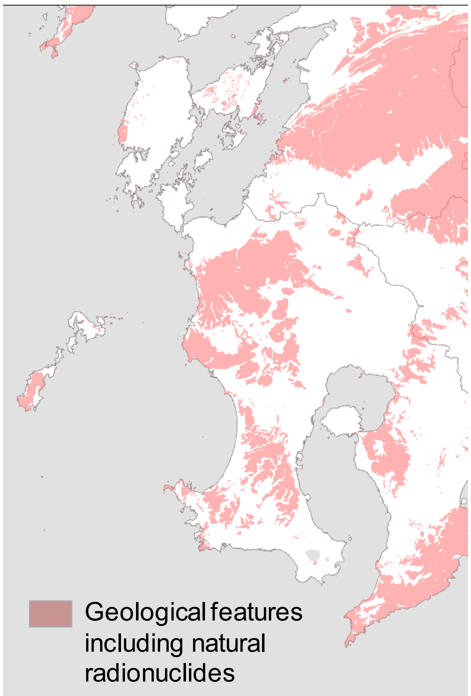

Fig. 8. Seamless digital geological map around the Sendai NPS (Geological Survey of Japan, AIST, 2015).

The colored areas are places containing large amounts of natural radionuclides.

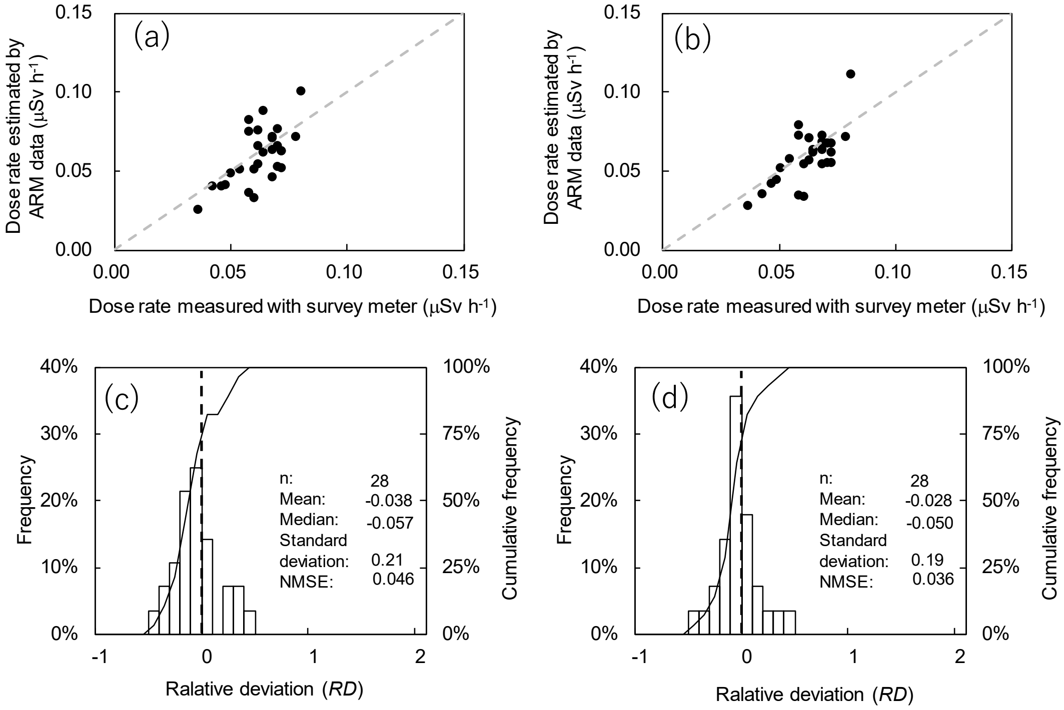

Fig. 9. Relation between the dose rates at a height of 1 m above the ground measured using a NaI survey meter and calculated from the ARM data around the Sendai NPS (a) before the discrimination (b) after the discrimination. Frequency distribution of relative deviation around the Sendai NPS (c) before the discrimination (d) after the discrimination.

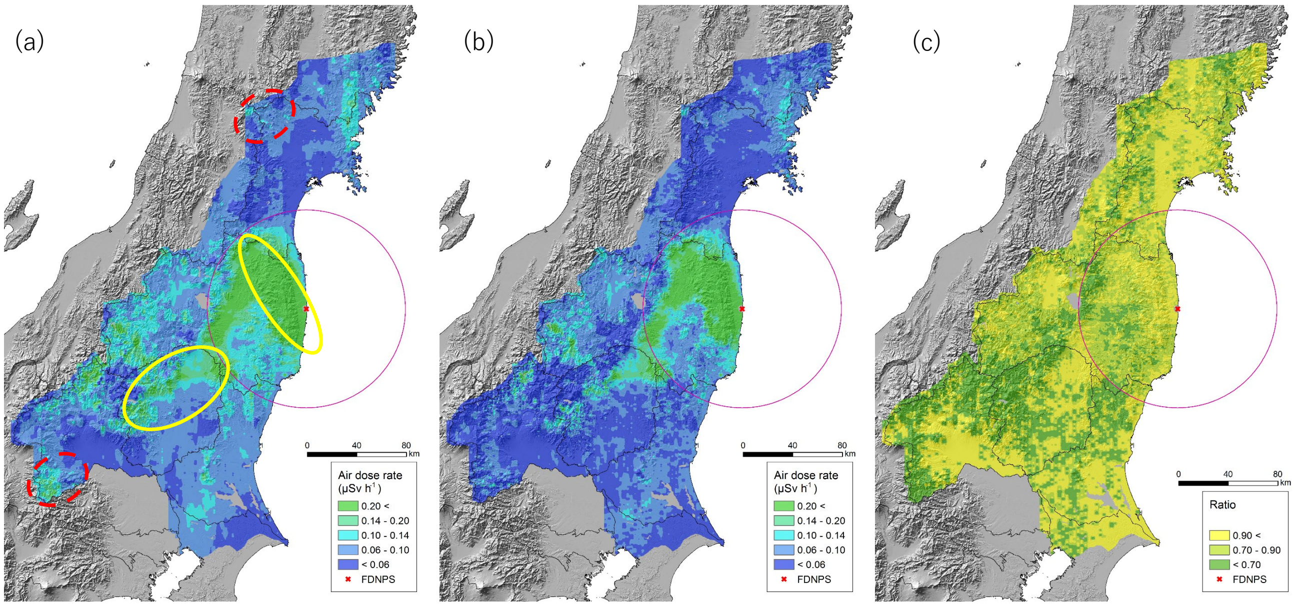

Fig. 10. Dose rate maps at a height of 1 m calculated from the ARM data around the Fukushima Dai-ichi NPS. (a) before the discrimination; (b) after the discrimination; (c) the ratio of (b) to (a).

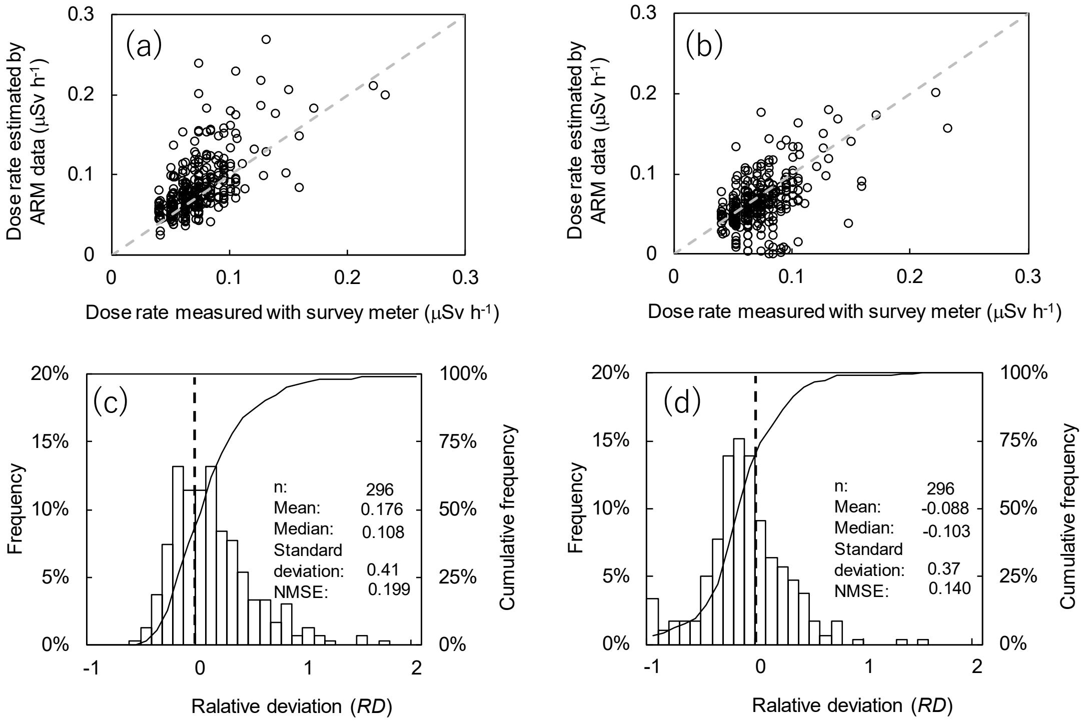

Fig. 11. Relation between the dose rates at a height of 1 m above the ground measured using a NaI survey meter and calculated from the ARM data around the Fukushima Dai-ichi NPS (a) before the discrimination (b) after the discrimination. Frequency distribution of relative deviation around the Fukushima Dai-ichi NPS (c) before the discrimination (d) after the discrimination.